# Chapter 4

## Isotopomer Fractionation in the UV Photolysis of $N_2O$: 2. Further Comparison of Theory and Experiment

[This chapter appeared in the *Journal of Geophysical Research-Atmospheres* **113**, D05309 (2008).]

JOURNAL OF GEOPHYSICAL RESEARCH, VOL. 113, D05309, doi:10.1029/2007JD009180, 2008

# Isotopomer fractionation in the UV photolysis of $N_2O$: 2. Further comparison of theory and experiment

Wei-Chen Chen,[1] Meher K. Prakash,[1] and R. A. Marcus[1]

Received 17 July 2007; revised 1 September 2007; accepted 18 December 2007; published 8 March 2008.

[1] Wavelength-dependent fractionation of various isotopomers in the photodissociation of $N_2O$ is studied. The absorption cross sections are calculated by a time-independent reflection principle, related to the Prakash et al. (2005) treatment but now with an inclusion of the NN stretching coordinate and both the $2A'$ and $1A''$ electronic excited states. The added $1A''$ state is found to have little effect on both the absorption cross section and the fractionation. The improvements include more physical details in the photodissociation of $N_2O$, while maintaining an advantage of a treatment in the work by Prakash et al. (2005) that was not computationally intensive. The present calculated fractionation, without a significant adjustable parameter, gives good agreement with experiments in the absorption cross section in the low-energy region, the important region for the experimentally observed isotopic fractionation.

**Citation:** Chen, W.-C., M. K. Prakash, and R. A. Marcus (2008), Isotopomer fractionation in the UV photolysis of $N_2O$: 2. Further comparison of theory and experiment, *J. Geophys. Res.*, *113*, D05309, doi:10.1029/2007JD009180.

## 1. Introduction

[2] The photolytic dissociation of molecules is important in stratospheric and atmospheric chemistry [e.g., *Wayne*, 2000]. $N_2O$, in particular, is an effective greenhouse gas and a source of $NO_x$. Isotopomer fractionation measurements help in determining the sources and sinks of atmospheric gases [*Stevens et al.*, 1972; *Brenninkmeijer et al.*, 2003]. The atmospheric modeling of the $N_2O$ isotopomers [*Popp et al.*, 2002; *Röckmann et al.*, 2003; *McLinden et al.*, 2003; *Morgan et al.*, 2004] and the isotopic fractionation photodissociation behavior of $N_2O$ [*Kim and Craig*, 1990; *Naqvi et al.*, 1998; *Brenninkmeijer et al.*, 2003; *Johnston et al.*, 1995] has been the subject of many studies, including wavelength-dependent measurements [*Zhang et al.*, 2000; *Turatti et al.*, 2000; *Röckmann et al.*, 2000, 2001; *Kaiser et al.*, 2003; *von Hessberg et al.*, 2004]. These studies motivated both empirical [*Blake et al.*, 2003; *Liang et al.*, 2004] and the more theoretical [*Johnson et al.*, 2001; *Nanbu and Johnson*, 2004; *Prakash et al.*, 2005] models to explain the wavelength-dependent fractionation.

[3] Frequently, the process is treated as a two-electronic-state process in which the lower electronic state is excited to the upper state by absorption of radiation [e.g., *Schinke*, 1993]. However, for polyatomic molecules, $N_2O$ being an example, there are usually a number of excited electronic states which are accessible even though the excitation to only one of them may be dominant in the wavelength region of interest. It has been convenient in such work to "broaden" the calculated absorption spectrum as a way of simulating the optical absorption into the other nearby electronic states, as in the treatment of the photolysis $N_2O$ in the work of *Daud et al.* [2005] Analogously, in the work by *Prakash et al.* [2005] (hereinafter referred to as part 1) such a broadening was included tacitly by using a scaling factor for the potential energy curve of the excited electronic state [*Prakash et al.*, 2005]. (The scale used for the excited state in the work by *Prakash et al.* [2005] was 1.57. The broadening there happened inadvertently and was not reported therein.)

[4] In the present paper, we extend the work of part 1 on $N_2O$ by including an effect of the changes in the NN bond length in $N_2O$, investigating the absorption to an additional electronic state, and using an absorption expression [*Heller*, 1978] that preserves both the momentum and coordinate parts of Franck-Condon principle. The calculated cross section without any broadening factor gives good agreement with experiment in the energy region of interest for the fractionation measurements (apart from a small shift of the absorption maximum). The fractionation of the various isotopomers is then obtained from these calculated absorption cross sections. We use the results of the vibrational analysis in part 1 to calculate the vibrational wave function in the ground state and then invoke the multidimensional reflection principle to calculate the absorption spectrum and the isotopic fractionation factors as a function of wavelength.

## 2. Theory

### 2.1. Absorption Cross Section

[5] The theoretical procedure used to obtain absorption cross sections for the $N_2O$ isotopomers is similar to that

[1]Noyes Laboratory, California Institute of Technology, Pasadena, California, USA.


0148-0227/08/2007JD009180$09.00

described previously by *Prakash et al.* [2005], but with some additions described below. UV photolysis of $N_2O$ is essentially a direct dissociation, since the shape of the absorption spectrum is a broad envelope with a only weak structure superimposed. Thereby, the time-dependent expression for the absorption cross section can be rewritten in a time-independent form using the reflection principle in conjunction with the Franck-Condon principle [*Heller*, 1978; *Schinke*, 1993]. The absorption cross section $\sigma$ is given as

$$\begin{aligned}\sigma_{f\nu}(\omega) &= \frac{\pi\omega}{\hbar\epsilon_0 c}\frac{1}{2\pi}\int_{\infty}^{-\infty} dt\langle\Psi_\nu|\vec{e}\cdot\vec{\mu}_{fi}^{\dagger}e^{-iH_f t/\hbar}\vec{\mu}_{fi}\cdot\vec{e}|\Psi_\nu\rangle e^{i(\omega-E_i/\hbar)t} \\ &\approx \frac{\pi\omega}{3\epsilon_0 c}\int d\mathbf{Q}|\Psi_\nu(\mathbf{Q})|^2|\vec{\mu}_{fi}(\mathbf{R})|^2\delta\big(\hbar\omega - V_f(\mathbf{R}) + V_i(\mathbf{R})\big) \\ &\approx \frac{\pi\omega}{3\epsilon_0 c}\int dq_1\ldots dq_{N-1}|\Psi_\nu(\mathbf{Q})|^2|\vec{\mu}_{fi}(\mathbf{Q})|^2/\Delta S, \qquad (1a)\end{aligned}$$

where a change in slope $\Delta S$ is given by

$$\Delta S = \big(\partial\big[V_i(\mathbf{Q}) - V_f(\mathbf{Q})\big]/\partial q_N\big)_{q_N^\omega}. \qquad (1b)$$

Here, $\mathbf{R}$ and $\mathbf{Q}$ denote internal and normal coordinates, respectively, as before [*Prakash et al.*, 2005], $\mathbf{R} = (q_1, q_2 \cdots q_N)$, $\vec{e}$ is a unit vector, $\vec{\mu}_{fi}(\mathbf{R})$ is the transition dipole moment function for a transition between the ground and the excited electronic states $i$ and $f$, respectively, $V_f(\mathbf{Q})$ and $V_i(\mathbf{Q})$ denote the potential energy surfaces of the electronic excited and ground states, respectively, and $q_N$ is the repulsive coordinate in the excited state $f$, along which dissociation happens, while $q_N^\omega$ in equation (1b) is the value of $q_N$ where $h\omega$ equals the vertical potential energy difference of the two electronic states:

$$\hbar\omega - V_f\big(q_1,\cdots,q_{N-1},q_N^\omega\big) + V_i\big(q_1,\cdots,q_{N-1},q_N^\omega\big) = 0, \qquad (2)$$

[6] $|\Psi_\nu(\mathbf{Q})|^2$ in equation (1a) is the probability density function of $\mathbf{Q}$ in the initial nuclear vibrational state $\nu$ and ground electronic state $i$. Using the harmonic approximation for the potential energy $V_i$ as a function of the normal coordinates, the probability density function of the vibrational state $\nu$ in the ground electronic state can be written as a product of that of each of the normal vibration modes.

[7] In the present calculation of the absorption cross section in equation (1b), the actual potential of the electronic ground state $V_i(\mathbf{Q})$ at coordinate $\mathbf{Q}$ is used [*Heller*, 1978], instead of the average potential energy $\langle V_i\rangle$ [*Lee et al.*, 1983; *Prakash et al.*, 2005]. This change corresponds to conserving the momenta in the Franck-Condon principle and enhances the calculated intensity of the absorption cross section on the long-wavelength side of absorption maximum. The result obtained with equation (1a) is shown and discussed later in section 3.1, now without any significant adjustable parameter. (The slope of the excited electronic potential in the work by *Prakash et al.* [2005] was enlarged by the broadening scale, which also increased the width of the absorption cross section.)

[8] The total absorption cross section is temperature-dependent, because of the dependence of $\sigma_{f\nu}$ on the initial vibrational state $\nu$ and thermal excitation of each vibrational states. The total absorption cross section at temperature $T$ is given by

$$\sigma_{total}(T) = \sum_{f,\nu}\sigma_{f\nu}\exp\left(\frac{-E_\nu}{k_B T}\right)/Q_{vib}(T), \qquad (3)$$

where $Q_{vib}(T)$ is the partition function of the vibrations in the ground electronic state, and $E_\nu$ is the vibrational energy of the vibrational state $\nu$. The present calculation for the total absorption cross section of $N_2O$ includes excitation from the ground electronic state to two excited states, $2A'$ ($1\Delta$) and $1A''$ ($1\Sigma^-$), and all vibrational states that are significantly populated with energy not more than 1500 $cm^{-1}$ above the zero-point energy. It involves the ground state, the first excited state of NO stretching, and the first and second excited states of the $N_2O$ bending. Since the $N_2O$ is linear in the electronic ground state, this bending vibration is doubly degenerate, as discussed in by *Prakash et al.* [2005].

### 2.2. Potential Energy

[9] The best currently available potential energy and transition dipole moment surfaces appear to be those of *Daud et al.* [2005] However, these surfaces are given in terms of mass-dependent Jacobi coordinates with a fixed NN distance. The present treatment of the potential energy surfaces includes varying the NN distance by expanding it to second-order in terms of a displacement of the equilibrium NN distance of both electronic ground and excited states. The details of the potential difference used in equation (1b) are given in Appendix A.

### 2.3. Fractionation

[10] The expression for the photodissociation rate at energy $h\omega$ in equation (1a) depends upon three factors: the total absorption cross section $\sigma_{total}(\omega)$ in equation (3), the photon flux, and the quantum yield of the photodissociation. The fractionation $\epsilon(\omega)$ of one isotopomer relative to another due to a direct photodissociation reaction can be defined as the ratio of photodissociation rates. When the upper state is dissociative, the quantum yield equals unity for all the isotopomers. The fractionation then is expressed in terms of the ratio of total absorption cross sections,

$$\epsilon(\omega) = \left[\frac{\sigma'_{total}(\omega)}{\sigma_{total}(\omega)} - 1\right]\times 1000\ ‰. \qquad (4)$$

## 3. Results and Discussion

### 3.1. Absorption Cross Section

[11] In the present treatment the potential difference between the ground and excited states in equation (1b) includes all vibrational modes of $N_2O$ in the calculation. A harmonic approximation is used in the NN stretching mode, which was fixed in the best currently available potential [*Daud et al.*, 2005]. The $N_2$ vibration is expected to be a spectator [*Hanisco and Kummel*, 1993; *Neyer et al.*, 1999] as far as the initial and final NN stretching state are concerned. The NN stretching mode is also expected to cause only a small change in the transition dipole moment of the $N_2O$ molecule. In the excited state, there is never-

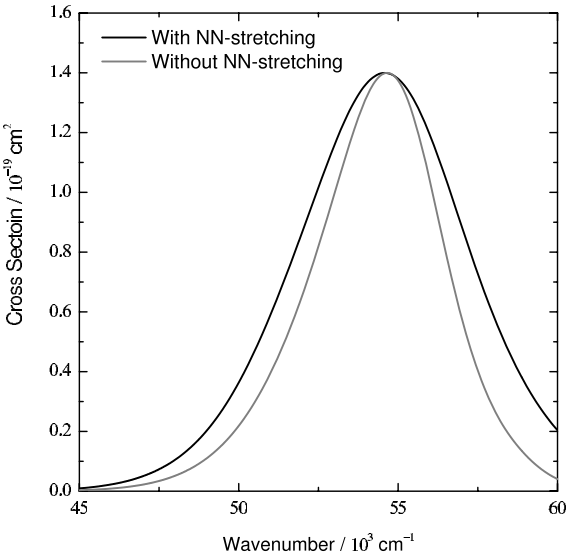


**Figure 1.** The calculated absorption cross section with (black) and without (gray) the NN stretching mode at 298 K.

theless a transient distortion of the NN coordinate because of the difference in $V_f(\mathbf{R})$ and $V_i(\mathbf{R})$ in this coordinate. Using an approximate method for introducing this distortion in Appendix A, there results a significant broadening effect in the absorption cross section, as shown in Figure 1. In this formalism, the NN stretching mode thus gives a broadening effect on the absorption cross section. The stored vibrational energy at the moment of excitation is relaxed to other modes

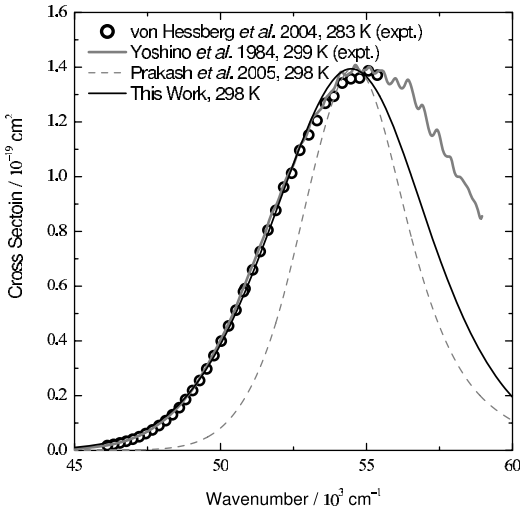


**Figure 2.** Absorption cross section of $^{14}N^{14}N^{16}O$. The black line is the current calculation result. The gray dashed line is the calculation result obtained by our previous formula [*Prakash et al.*, 2005], but without using any broadening factor. Both calculation results are rescaled and shifted to overlap their maximum absorption cross section at ~55000 cm$^{-1}$.

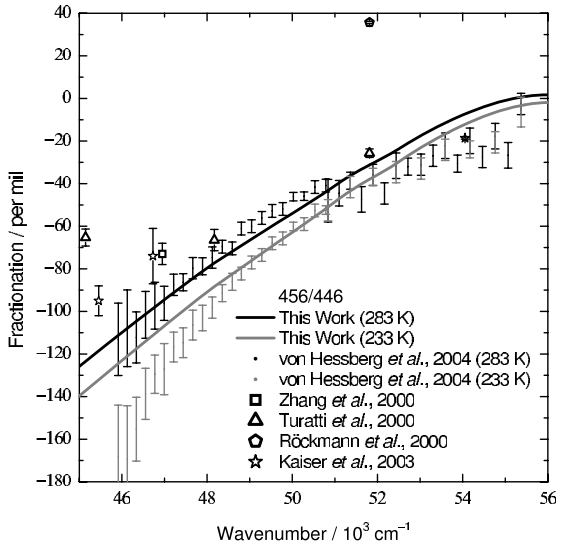


**Figure 3.** Fractionation of 456 calculated at 233 and 283 K.

later. The same Frank-Condon assumption was also used in the very accurate ionization-energy calculations in various molecules [*Cheng et al.*, 1997; *Eberhard et al.*, 1998], where it gives excellent results for the comparison of theory and experiment, now between vibrationally bound states. However, more detailed theoretical and experimental studies are necessary to test this assumption.

[12] The most important spectral region where isotopic fractionation studies of $N_2O$ have been reported is the long-wavelength side of the absorption maximum (180 nm to 220 nm). The calculated absorption cross section of the most abundant isotopomer, 446 (i.e., $^{14}N^{14}N^{16}O$), is compared with experiments [*Yoshino et al.*, 1984; *von Hessberg et al.*, 2004] in Figure 2, where the result calculated by our previous formula [*Prakash et al.*, 2005], but without their broadening factor, is also shown. The calculated properties needed to obtain the absorption cross section are provided in the Appendix C. In the comparison with the experimental spectrum, the calculated peak is red shifted by 1100 cm$^{-1}$ and rescaled by a factor of 0.69. The need for the shift arises from a small error in the difference between the energy of ground and excited electronic states from the ab initio calculations. Such differences are indeed expected. A rescaling in height is also expected since the ab initio calculation of the transition dipole moment $\vec{\mu}_{fi}$ is expected to have some errors [*Borges*, 2006; *Daud et al.*, 2005]. However, the rescaled factor at the absorption maximum has no effect on the isotopic fractionations since the factor cancels in equation (4). The total absorption cross sections for other isotopomers are calculated similarly with the same shift in the peak position as that for 446, since the energy difference between potential energy surfaces is independent of isotopic substitution. The red shifted value at the absorption maximum also has a minor red-shifted effect on the isotope fractionations.

[13] The agreement of calculated and measured absorption cross sections in Figure 2 is seen to be good on the long-wavelength side of absorption maximum, the region of

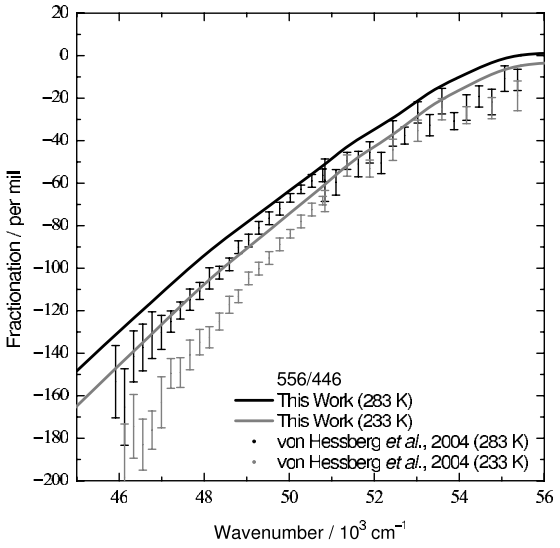


**Figure 4.** Fractionation of 556 calculated at 233 and 283 K.

most interest. In the short-wavelength side of the absorption spectrum the experimental result has larger cross section than the calculated. A difference is probably due to the presence of electronic excited states of $N_2O$ higher than $2A'$ and $1A''$, and perhaps due to the long tail in the cross section that involves the vibrationally excited NN stretching mode in the excited $N_2O$. Although that mechanism may broaden the absorption cross section at higher energy, it has little effect for the fractionation at the energies of conventional interest since there is less than 2% of products with the vibrationally excited $N_2$, *Hanisco and Kummel* [1993], and *Neyer et al.* [1999] both at ~200 nm, where the fractionations are of interests.

### 3.2. Wavelength-Dependent Fractionation

[14] The calculated wavelength-dependent fractionation of isotopomers 456, 556, and 546 relative to the most abundant isotopomer 446 are shown in Figures 3–5. The calculated values of 456 and 556 agree well with experimental data [*Zhang et al.*, 2000; *Turatti et al.*, 2000; *Röckmann et al.*, 2000, 2001; *Kaiser et al.*, 2003; *von Hessberg et al.*, 2004]. The values of 546 are not so good. Although the calculated fractionation 546 in Figure 5 is higher than the experimental result obtained by *von Hessberg et al.* [2004] at the long-wavelength region, our result is still comparable with the result observed by *Turatti et al.* [2000]. However, *Johnson et al.* [2001], using a completely different model (Hermite propagation method), obtained a fractionation 546 similar to ours. A more detailed theoretical study is necessary to see whether the discrepancy may be due to anharmonicity: the middle atom in 546 is the lightest and becomes the most susceptible to anharmonic effect (larger amplitude).

[15] Comparison with other ab initio values was given in part 1. Since the present calculations neglect the weak structure of the absorption cross section, the calculated fractionation is an averaged curve for comparison with the mean of the experiments. Compared with the previous paper [*Prakash et al.*, 2005], the current results agree better with experiments and now contain no ad hoc broadening factor is used. This improvement in the results over part 1 is expected since the current treatment includes some distortion effect of the NN stretching and also has a physically more understandable expression, equation (1a) and (1b), for the fractionation.

[16] The calculated fractionations 447 and 448 relative to 446 at 283 K is given in Figure 6. The agreement is very good [*Turatti et al.*, 2000; *Röckmann et al.*, 2000, 2001; *Kaiser et al.*, 2003]. Compared with fractionation of isotopomers, the sensitivity of the calculated fractionation to changes in the wavelength is 556 > 456 > 448 > 447 ~ 546. This trend is similar to the difference of the vibrational frequency of the bending mode between 446 and the respective isotopomers since the electronic excitation from the ground state to the excited state is forbidden for a linear $N_2O$. This transition is allowed only when the molecule is bent. In the experiments [*Zhang et al.*, 2000; *Turatti et al.*, 2000; *Röckmann et al.*, 2000, 2001; *Kaiser et al.*, 2003; *von Hessberg et al.*, 2004] the order is 556 > 456 > 448 ~ 546 > 447.

[17] All Figures 3–6 show a convex curve where the slope of wavelength-dependent fractionation decrease in the high-energy region. This result is different from that obtained by the empirical ZPE model [*Yung and Miller*, 1997], which predicts a straight line, because the model assumes that the slope of the absorption cross section is preserved upon isotope substitution. However, comparing the intensity factors, defined as the integral of the product of the vibrational probability function and the square of transition dipole moment, between 446 and various isotopomers, the factors have only a slight dependence on isotopomers (cf. Table 1). This dependence also should be important in the near leveling-off effect in the fractionation near the peak region of the absorption cross section. A similar calculational result is also discussed by *Johnson et al.* [2001]. (The intensity factor in the work by *Johnson et al.* [2001] is slightly different from ours.)

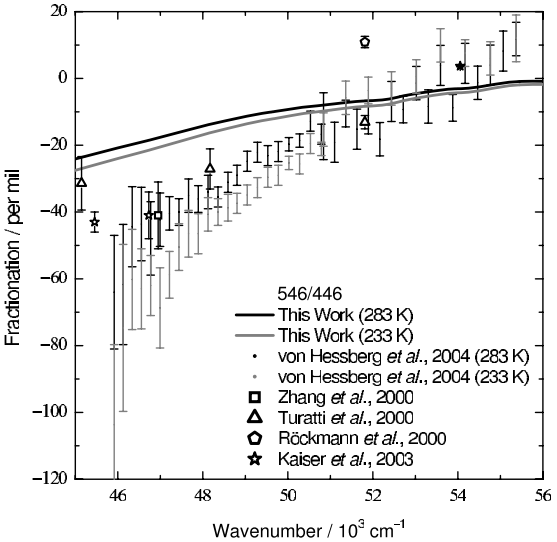


**Figure 5.** Fractionation of 546 calculated at 233 and 283 K.

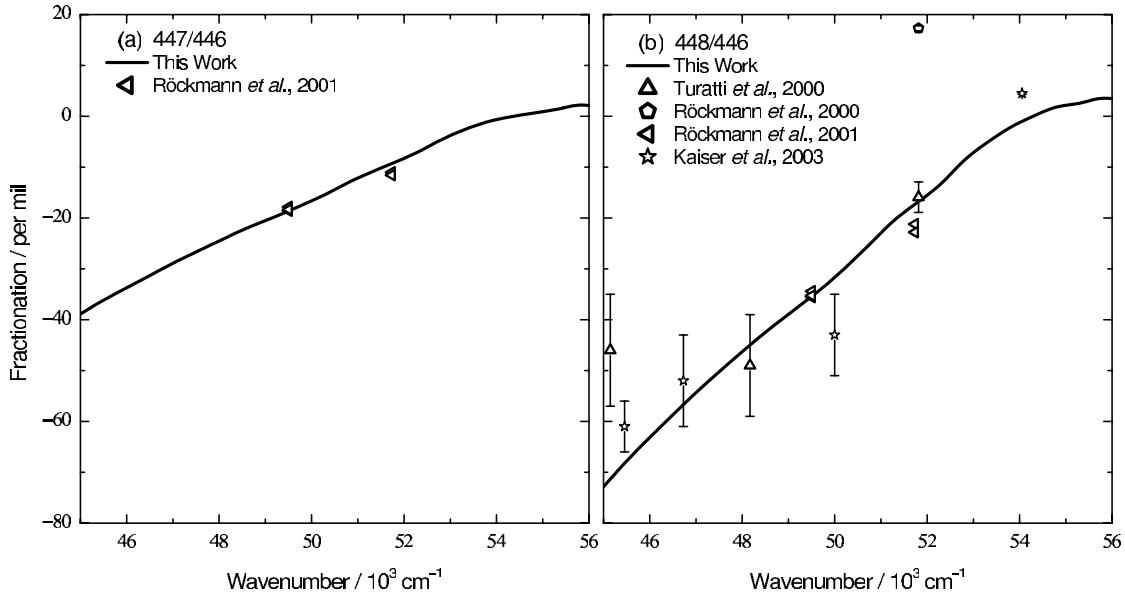


**Figure 6.** Fractionation of (a) 447 and (b) 448. The calculated values are at 283 K.

[18] There is a mass-dependent fractionation of oxygen isotopes in the current model, that is the same as the previous one [*Prakash et al.*, 2005; *Prakash and Marcus*, 2005]. This model also gives a mass-dependent fractionation in nitrogen fractionation, which is discussed elsewhere (W.-C. Chen and R. A. Marcus, Slopes in three-isotope plots of fractionation in photolysis of $N_2O$: A theory with reduced-mass approach, manuscript in preparation, 2008). The mass-dependent heavy oxygen isotope enrichment of residual $N_2O$ is also measured by *Johnston et al.* [1995]. The observation of anomalous mass effect of $N_2O$ in troposphere and lower stratosphere [*Cliff and Thiemens*, 1997; *Cliff et al.*, 1999; *Röckmann et al.*, 2001] is due to other chemical reactions, as discussed by *McLinden et al.* [2003] using a global model.

### 3.3. Excited Electronic States

[19] There are two potential energy surfaces ($2A'$ and $1A''$) included in these calculations. The $1A''$ state has a minor contribution in the calculation of absorption cross section since the peak intensity of the $1A''$ state is smaller than that of the $2A'$ state by a factor of $\sim$100. The intensity factor of various vibrational states of the isotopomer 446 is shown in Table 1. This difference in intensity is similar to that found in the time-dependent calculation by *Daud et al.* [2005]. It also has a very minor contribution (<2 per mil) to the fractionation of all isotopomers. Since the effect of the $1A''$ state is very small, we do not show the results in figures.

## 4. Conclusions

[20] The absorption cross section of 446 calculated using a computationally simple time-independent treatment with small adjustments for the position of the peak and its amplitude is in reasonable agreement with the broad envelope of the cross section in experiments. (Compared with the wave packet propagation method, the current method requires less computational resources. Both methods depend heavily on accurate transition dipole moment and potential energy surfaces of the electronic ground and excited states, which is not a simple task.) The required computations are similar to that in our previous treatment [*Prakash et al.*, 2005] but there are several improvements in the calculations, including the effect of NN stretching and avoiding the need for an empirical broadening parameter. There is a reasonable agreement in the wavelength-dependent fractionations of the isotopomers. The $2A'$ excited state dominates both the absorption cross section and fractionation in the $N_2O$ photodissociation.

**Table 1.** Intensity Factors of 446 in the Various Vibrational States and the Ratio of Intensity Factors Between 446 and Other Isotopomers[a]

| | 000 | 001 | 002 | 010 |
|---|---|---|---|---|
| | | $2A'$ | | |
| 446 | 7.561 | 16.58[b] | 24.41[c] | 8.1493 |
| 447/446 | 0.9934 | 0.9949 | 0.9954 | 0.9923 |
| 448/446 | 0.9880 | 0.9903 | 0.9915 | 0.9858 |
| 456/446 | 0.9708 | 0.9760 | 0.9788 | 0.9714 |
| 546/446 | 0.9923 | 0.9939 | 0.9944 | 0.9895 |
| 556/446 | 0.9637 | 0.9702 | 0.9739 | 0.9614 |
| | | $1A''$ | | |
| 446 | 0.08755 | 0.1489[b] | 0.1787[c] | 0.1760 |
| 447/446 | 0.9831 | 0.9848 | 0.9856 | 0.9866 |
| 448/446 | 0.9684 | 0.9713 | 0.9729 | 0.9746 |
| 456/446 | 0.9710 | 0.9764 | 0.9813 | 0.9833 |
| 546/446 | 0.9948 | 0.9963 | 0.9973 | 0.9764 |
| 556/446 | 0.9662 | 0.9727 | 0.9788 | 0.9598 |

[a]The vibrational quantum states are denoted as a three-digit number, such as 001, in which the digits indicate the vibrational quantum number of $\nu_1$, $\nu_2$, and $\nu_3$, respectively. The vibrational frequencies of various isotopomers are listed in Table 2. The unit of intensity factors is $10^{-3}$ (atomic unit)$^2$.
[b]An average value of two degenerate vibrational states.
[c]An average value of three degenerate vibrational states.

[21] The current method is useful for studying isotopic fractionation in direct photodissociation systems when accurate transition moment and potential energy surfaces are available. However, other interesting photodissociation reactions, such as ozone, $CO_2$, and OCS, have a trapped state before dissociation or involve more than one excited states in the photodissociation process. In order to study these more complicated photodissociation, further developments on the current theory are required. When the quantum yield for dissociation is close to unity, then it is possible that the present method can be adapted to these other systems.

## Appendix A: Potential Energy Difference

[22] The potential difference in equation (1b) is expanded as

$$V_f(\mathbf{R}) - V_i(\mathbf{R}) \approx V_f(\mathbf{\Gamma}) + \frac{1}{2}k_{N_2}\left[(r_{NN} - r_\Delta)^2 - r_\Delta^2\right] - V_i(\mathbf{\Gamma}) - \frac{1}{2}k_{NN,NN}r_{NN}^2 - \frac{1}{2}k_{NO,NO}r_{NO}^2 - k_{NN,NO}r_{NN}r_{NO}, \tag{A1}$$

where $r_{NN}$ and $r_{NO}$ are the displacement of the NN and NO distances, respectively, from the equilibrium at the electronic ground state, and $r_\Delta$ is the difference in the equilibrium NN distance between $N_2$ and $N_2O$. Because in the excited state the $N_2$ formed a triple bond, and the NO coordinate is a strongly repulsive one, the force constant corresponding to the cross terms of $r_{NN}$ and $r_{NO}$ is assumed to be small compared with these two dominate coordinates on the excited state potential energy surfaces. A further detailed calculation about this coupling on the excited potential energy surface is needed to validate this assumption. In equation (A1), $\mathbf{\Gamma}$ has the same meaning as $\mathbf{R}$, but with the displacement coordinate $r_{NN} = 0$; The integration in equation (1a) is more easily performed in normal coordinates. The relation between internal and normal coordinates satisfies $\mathbf{R} = \mathscr{L}\mathbf{Q}$, where $\mathscr{L}$ is a matrix composed of eigenvectors of the $\mathcal{GF}$ matrix [*Wilson et al.*, 1955]. The $\mathcal{G}$ and $\mathcal{F}$ matrices of $N_2O$ are given in Appendix B. The potential difference is rewritten as

$$\begin{aligned} V_f(\mathbf{R}) - V_i(\mathbf{R}) &= V_f(\mathbf{Q}) - V_i(\mathbf{Q}) \\ &\approx V_f\left(0, L_{2,i}q_i, L_{3,3}q_3\right) + \frac{1}{2}k_{N_2}\left[\left(L_{1,i}q_i - r_\Delta\right)^2 - r_\Delta^2\right] \\ &\quad - V_i\left(0, L_{2,i}q_i, L_{3,3}q_3\right) - \frac{1}{2}\omega_1^2\left[q_1^2 - \left(L_{1,2}^{-1}L_{2,i}q_i\right)^2\right] \\ &\quad - \frac{1}{2}\omega_2^2\left[q_2^2 - \left(L_{2,2}^{-1}L_{2,i}q_i\right)^2\right], \end{aligned} \tag{A2}$$

where $\sum_{i=1}^{2} L_{j,i}q_i$ are abbreviated as $L_{j,i}q_i$, and $L_{i,j}$ and $L_{i,j}^{-1}$ are the ($i$th, $j$th) elements of the matrices $\mathscr{L}$ and $\mathscr{L}^{-1}$, respectively.

[23] A treatment of the NN distance contribution to the vibration is in one sense different from that of the NO coordinate. Unlike the NO coordinate it is not a dissociative one. However, because of the difference in the NN contribution to the two potential energy functions $V_f$ and $V_i$ in the two electronic states, and the coupling of the motion to the NO coordinate, the NN coordinate is not a bystander, even though the product is formed primarily in the $N_2$ ground vibrational state, and $N_2O$ is a almost entirely in the lowest NN stretching vibrational state before illumination. For simplicity, we have used the simple Frank-Condon assumption given above and used successfully earlier by *Cheng et al.* [1997] and *Eberhard et al.* [1998] in the studies of the vertical ionization energy (rather than an absorption spectrum). The molecules studied in the neutral and cation state have the same chemical formula (except for the charge of the state), although their equilibrium geometries are slightly different. However, ultimately the model should be compared with more rigorous treatment. The present method recognizes a distortion that occurs in the NN vibration, due to differences in $V_f(\mathbf{R})$ and $V_i(\mathbf{R})$ for that coordinate, and so by this distortion transiently stores energy in that coordinate and so broadens the absorption spectrum.

## Appendix B: $\mathcal{G}$ and $\mathcal{F}$ Matrices

[24] The $\mathcal{G}$ and $\mathcal{F}$ matrices of $N^1N^2O$ are defined as [*Wilson et al.*, 1955]

$$\mathcal{G} = \begin{pmatrix} \frac{1}{m_{N^1}} + \frac{1}{m_{N^2}} & \frac{-1}{m_{N^2}} & 0 \\ \frac{-1}{m_{N^2}} & \frac{1}{m_{N^2}} + \frac{1}{m_O} & 0 \\ 0 & 0 & \frac{1}{m_{N^1}\left(r_{NN}^{eq}\right)^2} + \frac{1}{m_{N^2}}\left(\frac{1}{r_{NN}^{eq}} + \frac{1}{r_{NO}^{eq}}\right)^2 + \frac{1}{m_O\left(r_{NO}^{eq}\right)^2} \end{pmatrix}, \tag{B1}$$

$$\mathcal{F} = \begin{pmatrix} k_{NN,NN} & k_{NN,NO} & 0 \\ k_{NN,NO} & k_{NO,NO} & 0 \\ 0 & 0 & k_{\theta,\theta} \end{pmatrix}. \tag{B2}$$

The mass of each isotope are available from *Lide* [2004]. The equilibrium NN and NO distance for $N_2O$ is 1.1273 and 1.1851 Å, respectively, which are obtained experimentally by *Teffo and Chédin* [1989]. The force constants of the $\mathcal{F}$ matrix are given in Appendix C. The $\mathcal{L}$ matrix is obtained by solving the eigenvectors of the $\mathcal{GF}$ matrix.

## Appendix C: Properties of Isotopomers

[25] This appendix provides the parameters used for obtaining the absorption cross section of various isotopomers. The mass of each isotope are available from *Lide* [2004]. The equilibrium bond length for $N_2$ is 1.09768 Å (http://webbook.nist.gov/cgi/cbook.cgi?Formula=n2&NoIon=on&Units=SI&cDI=on). The force constant in the ground state $k_{N2}$ is 22.948 aJ/Å$^2$. The force constants for

**Table A1.** Calculated and Experimental Normal-Mode Frequencies of Various Isotopomers[a]

| | $\bar{\nu}_1$ | $\bar{\nu}_1^{expt.b}$ | $\bar{\nu}_2$ | $\bar{\nu}_2^{expt.c}$ | $\bar{\nu}_3$ | $\bar{\nu}_3^{expt.d}$ |
|---|---|---|---|---|---|---|
| 446 | 2224.424 | 2223.757 | 1286.003 | 1284.903 | 588.729 | 588.768 |
| 447 | 2221.012 | 2220.074 | 1263.532 | 1264.704 | 586.264 | 586.362 |
| 448 | 2218.085 | 2216.711 | 1243.136 | 1246.885 | 584.074 | 584.225 |
| 456 | 2176.677 | 2177.657 | 1284.090 | 1280.354 | 575.272 | 575.434 |
| 546 | 2201.880 | 2201.605 | 1269.392 | 1269.892 | 585.225 | 585.312 |
| 556 | 2153.347 | 2154.726 | 1267.940 | 1265.334 | 571.685 | 571.894 |

[a]Unit is $cm^{-1}$.
[b]*Toth* [1986].
[c]*Amiot* [1976] and *Jolma et al.* [1983].
[d]*Toth* [1987].

$N_2O$ are $k_{NN,NN}$ = 17.655 aJ/Å$^2$; $k_{NO,NO}$ = 11.559 aJ/Å$^2$; $k_{NN,NO}$ = 1.260 aJ/Å$^2$; and $k_{\theta,\theta}$ = 0.649 aJ/rad$^2$ [*Csaszar*, 1994]. The force constants are calculated by fitting the experimental vibrational frequencies of various $N_2O$ isotopomers. The difference between calculated and experimental frequencies, as shown in Table A1, are smaller than $\pm 3.7$ $cm^{-1}$ in the two stretching modes and $\pm 0.3$ $cm^{-1}$ in the bending mode. The force constants used in the present work are slightly different from the experimental values obtained by *Teffo and Chédin* [1989], used in our previous work [*Prakash et al.*, 2005].

[26] **Acknowledgment.** It is a pleasure to acknowledge the support of this research by the National Science Foundation.

## References

Amiot, C. (1976), Vibration-rotation bands of $^{15}N_2{}^{16}O$-$^{14}N_2{}^{18}O$, *J. Mol. Spectrosc.*, *59*(3), 380–395.

Blake, G. A., M. C. Liang, C. G. Morgan, and Y. L. Yung (2003), A Born-Oppenheimer photolysis model of $N_2O$ fractionation, *Geophys. Res. Lett.*, *30*(12), 1656, doi:10.1029/2003GL016932.

Borges, I. (2006), Configuration interaction oscillator strengths of the H2O molecule: Transitions from the ground to the $B^1A_1$, $C^1B_1$, $D^1A_1$, and $1^1B_2$ excited states, *Chem. Phys.*, *328*(1–3), 284–290.

Brenninkmeijer, C. A. M., C. Janssen, J. Kaiser, T. Röckmann, T. S. Rhee, and S. S. Assonov (2003), Isotope effects in the chemistry of atmospheric trace compounds, *Chem. Rev.*, *103*(12), 5125–5161.

Cheng, B. M., J. Eberhard, W. C. Chen, and C. H. Yu (1997), Photoionization efficiency spectrum and ionization energy of HSO studied by discharge flow photoionization mass spectrometry, *J. Chem. Phys.*, *106*(23), 9727–9733.

Cliff, S. S., and M. H. Thiemens (1997), The $^{18}O/^{16}O$ and $^{17}O/^{16}O$ ratios in atmospheric nitrous oxide: A mass-independent anomaly, *Science*, *278*(5344), 1774–1776.

Cliff, S. S., C. A. M. Brenninkmeijer, and M. H. Thiemens (1999), First measurement of the $^{18}O/^{16}O$ and $^{17}O/^{16}O$ ratios in stratospheric nitrous oxide: A mass-independent anomaly, *J. Geophys. Res.*, *104*, 16,171–16,175.

Csaszar, A. G. (1994), Anharmonic force field of $N_2O$, *J. Phys. Chem.*, *98*(36), 8823–8826.

Daud, M. N., G. G. Balint-Kurti, and A. Brown (2005), Ab initio potential energy surfaces, total absorption cross sections, and product quantum state distributions for the low-lying electronic states of $N_2O$, *J. Chem. Phys.*, *122*(5), 054305.

Eberhard, J., W. C. Chen, C. H. Yu, Y. P. Lee, and B. M. Cheng (1998), Photoionization spectra and ionization energies of HSCl, HSSSH, SSCl, and HSSCl formed in the reaction system $Cl/Cl_2/H_2S$, *J. Chem. Phys.*, *108*(15), 6197–6204.

Hanisco, T. F., and A. C. Kummel (1993), State-resolved photodissociation of $N_2O$, *J. Phys. Chem.*, *97*(28), 7242–7246.

Heller, E. J. (1978), Quantum corrections to classical photo-dissociation models, *J. Chem. Phys.*, *68*(5), 2066–2075.

Johnson, M. S., G. D. Billing, A. Gruodis, and M. H. M. Janssen (2001), Photolysis of nitrous oxide isotopomers studied by time-dependent Hermite propagation, *J. Phys. Chem. A*, *105*(38), 8672–8680.

Johnston, J. C., S. S. Cliff, and M. H. Thiemens (1995), Measurement of multioxygen isotopic ($\delta^{18}O$ and ($\delta^{17}O$) fractionation factors in the stratospheric sink reactions of nitrous-oxide, *J. Geophys. Res.*, *100*, 16,801–16,804.

Jolma, K., J. Kauppinen, and V. M. Horneman (1983), Vibration-rotation spectrum of $N_2O$ in the region of the lowest fundamental $\nu_2$, *J. Mol. Spectrosc.*, *101*(2), 278–284.

Kaiser, J., T. Röckmann, C. A. M. Brenninkmeijer, and P. J. Crutzen (2003), Wavelength dependence of isotope fractionation in $N_2O$ photolysis, *Atmos. Chem. Phys.*, *3*, 303–313.

Kim, K. R., and H. Craig (1990), 2-isotope characterization of $N_2O$ in the Pacific Ocean and constraints on its origin in deep-water, *Nature*, *347*(6288), 58–61.

Lee, S. Y., R. C. Brown, and E. J. Heller (1983), Multidimensional reflection approximation—Application to the photo-dissociation of polyatomics, *J. Chem. Phys.*, *87*(12), 2045–2053.

Liang, M. C., G. A. Blake, and Y. L. Yung (2004), A semianalytic model for photo-induced isotopic fractionation in simple molecules, *J. Geophys. Res.*, *109*, D10308, doi:10.1029/2004JD004539.

Lide, D. R. (Ed.) (2004), *CRC Handbook of Chemistry and Physics*, 84th ed., CRC Press, Boca Raton, Fla.

McLinden, C. A., M. J. Prather, and M. S. Johnson (2003), Global modeling of the isotopic analogues of $N_2O$: Stratospheric distributions, budgets, and the $^{17}O$-$^{18}O$ mass-independent anomaly, *J. Geophys. Res.*, *108*(D8), 4233, doi:10.1029/2002JD002560.

Morgan, C. G., M. Allen, M. C. Liang, R. L. Shia, G. A. Blake, and Y. L. Yung (2004), Isotopic fractionation of nitrous oxide in the stratosphere: Comparison between model and observations, *J. Geophys. Res.*, *109*, D04305, doi:10.1029/2003JD003402.

Nanbu, S., and M. S. Johnson (2004), Analysis of the ultraviolet absorption cross sections of six isotopically substituted nitrous oxide species using 3d wave packet propagation, *J. Phys. Chem. A*, *108*(41), 8905–8913.

Naqvi, S. W. A., T. Yoshinari, D. A. Jayakumar, M. A. Altabet, P. V. Narvekar, A. H. Devol, J. A. Brandes, and L. A. Codispoti (1998), Budgetary and biogeochemical implications of $N_2O$ isotope signatures in the Arabian Sea, *Nature*, *394*(6692), 462–464.

Neyer, D. W., A. J. R. Heck, and D. W. Chandler (1999), Photodissociation of $N_2O$: J-dependent anisotropy revealed in $N_2$ photofragment images, *J. Chem. Phys.*, *110*(7), 3411–3417.

Popp, B. N., et al. (2002), Nitrogen and oxygen isotopomeric constraints on the origins and sea-to-air flux of $N_2O$ in the oligotrophic subtropical North Pacific gyre, *Global Biogeochem. Cycles*, *16*(4), 1064, doi:10.1029/2001GB001806.

Prakash, M. K., and R. A. Marcus (2005), Three-isotope plot of fractionation in photolysis: A perturbation theoretical expression, *J. Chem. Phys.*, *123*(17), 174308.

Prakash, M. K., J. D. Weibel, and R. A. Marcus (2005), Isotopomer fractionation in the UV photolysis of $N_2O$: Comparison of theory and experiment, *J. Geophys. Res.*, *110*, D21315, doi:10.1029/2005JD006127.

Röckmann, T., C. A. M. Brenninkmeijer, M. Wollenhaupt, J. N. Crowley, and P. J. Crutzen (2000), Measurement of the isotopic fractionation of $^{15}N^{14}N^{16}O$, $^{14}N^{15}N^{16}O$ and $^{14}N^{14}N^{18}O$ in the UV photolysis of nitrous oxide, *Geophys. Res. Lett.*, *27*(9), 1399–1402.

Röckmann, T., J. Kaiser, J. N. Crowley, C. A. M. Brenninkmeijer, and P. J. Crutzen (2001), The origin of the anomalous or "mass-independent" oxygen isotope fractionation in tropospheric $N_2O$, *Geophys. Res. Lett.*, *28*(3), 503–506.

Röckmann, T., J. Kaiser, and C. A. M. Brenninkmeijer (2003), The isotopic fingerprint of the pre-industrial and the anthropogenic $N_2O$ source, *Atmos. Chem. Phys.*, *3*, 315–323.

Schinke, R. (1993), *Photodissociation Dynamics*, Cambridge Univ. Press, New York.

Stevens, C. M., D. Walling, A. Venters, L. E. Ross, A. Engelkem, and L. Krout (1972), Isotopic composition of atmospheric carbon-monoxide, *Earth Planet. Sci. Lett.*, *16*(2), 147–165.

Teffo, J. L., and A. Chédin (1989), Internuclear potential and equilibrium structure of the nitrous-oxide molecule from rovibrational data, *J. Mol. Spectrosc.*, *135*(5), 389–409.

Toth, R. A. (1986), Frequencies of $N_2O$ in the 1100 $cm^{-1}$ to 1440 $cm^{-1}$ region, *J. Opt. Soc. Am. B*, *3*(10), 1263–1281.

Toth, R. A. (1987), $N_2O$ vibration-rotation parameters derived from measurements in the 900–1090 $cm^{-1}$ and 1580–2380 $cm^{-1}$ regions, *J. Opt. Soc. Am. B*, *4*(3), 357–374.

Turatti, F., D. W. T. Griffith, S. R. Wilson, M. B. Esler, T. Rahn, H. Zhang, and G. A. Blake (2000), Positionally dependent $^{15}N$ fractionation factors in the UV photolysis of $N_2O$ determined by high resolution FTIR spectroscopy, *Geophys. Res. Lett.*, *27*(16), 2489–2492.

von Hessberg, P., J. Kaiser, M. B. Enghoff, C. A. McLinden, S. L. Sorensen, T. Röckmann, and M. S. Johnson (2004), Ultra-violet absorption cross sections of isotopically substituted nitrous oxide species: $^{14}N^{14}NO$, $^{15}N^{14}NO$, $^{14}N^{15}NO$ and $^{15}N^{15}NO$, *Atmos. Chem. Phys.*, *4*(41), 1237–1253.

Wayne, R. P. (2000), *Chemistry of Atmospheres*, 3rd ed., Oxford Univ. Press, New York.

Wilson, E. B., J. C. Decius, and P. C. Cross (1955), *Molecular Vibrations: The Theory of Infrared and Raman Vibrational Spectra*, McGraw-Hill, New York.

Yoshino, K., D. E. Freeman, and W. H. Parkinson (1984), High-resolution absorption cross-section measurements of $N_2O$ at 295 K–299 K in the wavelength region 170–222 nm, *Planet. Space Sci.*, *32*(10), 1219–1222.

Yung, Y. L., and C. E. Miller (1997), Isotopic fractionation of stratospheric nitrous oxide, *Science*, *278*(5344), 1778–1780.

Zhang, H., P. O. Wennberg, V. H. Wu, and G. A. Blake (2000), Fractionation of $^{14}N^{15}N^{16}O$ and $^{15}N^{14}N^{16}O$ during photolysis at 213 nm, *Geophys. Res. Lett.*, *27*(16), 2481–2484.

W.-C. Chen, R. A. Marcus, and M. K. Prakash, Noyes Laboratory 127-72, California Institute of Technology, Pasadena, CA 91125, USA. (cwc@caltech.edu; ram@caltech.edu; meher@caltech.edu)